Chinese Science Bulletin

Progress and prospect for high temperature single-phased magnetic ferroelectrics

YU Jian[1,2†] & CHU JunHao[2]

[1] Functional Materials Research Laboratory, Tongji University, Shanghai 200092, China;
[2] National Laboratory for Infrared Physics, Shanghai Institute of Technical Physics, Chinese Academy of Sciences, Shanghai 200083, China

Magnetic ferroelectrics are one of the most important functional materials. The present bottleneck limiting applications of them is lacking of high-temperature single-phased ferromagnetic-ferroelectric multiferroics with strong magnetoelectric coupling effect. Here, those progresses of the mechanism for coexistence of ferroelectric and magnetic order, experimental and theoretical studies on single-phased magnetic ferroelectrics, and the relationship between magnetic structure and crystal symmetry are summarized. With examples of $BiFeO_3$, $BiMnO_3$ and Bi_2FeCrO_6, the difficulties encountered in this field are analyzed. At last, some prospects to develop high-temperature single-phased ferromagnetic-ferroelectric multiferroics are also presented.

multiferroics, magnetoelectric effect, single-phased compound, magnetic ferroelectrics, high ordering temperature, $BiFeO_3$, $BiMnO_3$, Bi_2CrFeO_6

Magnetoelectric multiferroics not only exhibit the performances of both ferromagnetism and ferroelectricity, but also the magnetoelectric coupling effect—magnetic (electric) field induction of polarization P (magnetization M), which was first predicted by Curie in 1894 and confirmed in 1959–1960 theoretically by Dzyaloshinsky[1] and experimentally in the Cr_2O_3 by Astrov[2]. Since then, multiferroic and magnetoelectric materials have been attracting an increasing fundamental and practical interest. For example, they have high dielectric permittivity and high magnetic permeability, and could therefore replace the inductor and capacitor in resonant circuits with a single component, further miniaturize portable cellular technologies. Strong coupling between the polarization and magnetization would allow ferroelectric data storage combined with a magnetic read and the ability to tune or switch the magnetic properties with an electric field, and vice versa, could lead to as-yet unanticipated developments in conventional devices such as transducers.

The attempts to combine in one single-phased system both ferromagnetic and ferroelectric ordering states started in the 1960s, predominantly by Smolenskii and his co-worker[3,4]. The first ferromagnetic ferroelectric material to be discovered is nickel iodine boracite, $Ni_3B_7O_{13}I$, with magnetic ordering below $T_C = 60$ K and ferroelectric one below $T_C = 400$ K. The succeeding search for other ferromagnetic ferroelectrics began with the strategy of replacing some of the B-site d^0 cations in the ferroelectric perovskite oxides by magnetic d^n cations, and there were disclosed B-site ordered ferroelectric ferrimagnetic $Pb(Fe_{2/3}W_{1/3})O_3$, B-site disordered ferroelectric antiferromagnetic $Pb(Fe_{1/2}Ta_{1/2})O_3$ and $Pb(Fe_{1/2}Nb_{1/2})O_3$. $Pb(Fe_{2/3}W_{1/3})O_3$ crystallizes in the cubic at room temperature with space group *Pm3m* and lattice constant $a = 3.98$ Å, and shows very weak 1:1

Received December 19, 2007; accepted April 15, 2008
doi: 10.1007/s11434-008-0308-3
†Corresponding author (email: jyu@mail.tongji.edu.cn)
Partially supported by the National Natural Science Foundation of China (Grant No. 10304021), National Basic Research Program of China (Grant No. 2007CB924900), Foundation for the Author of National Excellent Doctoral Dissertation of China (FANEDD-200744), Shanghai Pujiang Program (Grant No. 07pj14087) and Program for New Century Excellent Talents in University (NCET-07-0624)

cation order limited to the nanometer scale of about 5 nm. It becomes ferrimagnetic ordering below T_C = 406 K (calculated) and 383 K (experimental) and ferroelectric one below T_{max} = 190 K (experimental)[5,6]. To increase saturation magnetization, it has been attempted to enhance the long range B-site cation ordering through doping Mg^{2+} and Co^{2+} and forming solid solution with high ordered $Pb(Sc_{2/3}W_{1/3})O_3$. Substitution of Fe with Sc, the cation order in the $Pb(Fe_{2/3}W_{1/3})O_3$ was enhanced, demonstrated by the strengthening of $\left(\frac{1}{2}\frac{1}{2}\frac{1}{2}\right)$-type superlattice peaks, and the maximum saturation magnetization obtained as 0.61 μ_B per ABO_3 formula for 15% substitution[6]. Another interesting case is the simple perovskite-type $BiFeO_3$. It contains only magnetic transition metal ions Fe^{3+} (d^5) on the B-site but has been demonstrated exhibiting both ferroelectric and magnetic orderings. It is of interest to note that $BiFeO_3$ is well known only prototypical material with both magnetic and ferroelectric ordering temperatures above room temperature.

So far, more than two hundred kinds of single-phased compounds are disclosed to be multiferroicism. However, the vast majority of them have low magnetic ordering temperature or exhibit character of antiferromagnetism or weak ferromagnetism, or are not strong enough insulators to sustain a ferroelectric polarization at room temperature, and the magnitude of the observed magnetoelectric effect is too small to apply for any practical devices[7]. According to the phenomenological theory, the magnetoelectric response α_{ij} of a single-phased material is limited by dielectric constant ε_{ii} and magnetic permeability μ_{jj} through the relationship

$$\alpha_{ij}^2 < \varepsilon_{ii}\mu_{jj}.$$

Therefore the multiferroic materials with large and robust ferromagnetic and ferroelectric ordering will have large magnetoelectric coupling effect, to obtain such multiferroic single-phased compound is still a challenge, in particular with both high ordering temperatures.

In this article, we will concentrate on reviewing those progresses and difficulties encountered in designing and developing high-temperature single-phased multiferroic compounds and provide some considerations during their attempting.

1 Production of ferroelectricity

Because of the simplicity of the structure and their actual or potential applications, perovskite-type ABO_3 (shown in Figure 1) and their derivatives are amongst the most studied compounds in solid state science for ferroelectricity, magnetism, superconducting, colossal magnetoresistance and multiferroicism. Despite decades of studies, the mechanisms of these phase transitions are still a matter of debate. It is the case of the oxygen perovskites, such as $SrTiO_3$ and $KTaO_3$, which only exhibit incipient ferroelectricity, while $PbTiO_3$, $BaTiO_3$ and $KNbO_3$ stabilize this instability in well-de- fined series of ferroelectric transitions; $BiFeO_3$ is an antiferromagnetic with complex spatial spin modulation structure while $BiMnO_3$ is ferromagnetic. Any progress in understanding the microscopic mechanism of electric and/or magnetic instabilities would promote one's attempt to design and develop high temperature single-phased ferromagnetic and ferroelectric multiferroic materials.

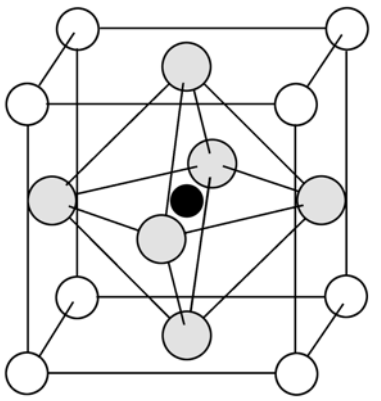

Figure 1 The perovskite structure. The small B cation (in black) is at the center of an octahedron of oxygen anions (in gray). The large A cations (white) occupy the unit cell corners.

To make novel magnetic ferroelectrics, in particular high temperature single-phased compounds, various kinds of mechanism of coexistence of magnetic and ferroelectric ordering have been intensively investigated. The ongoing researches are being mostly concentrated on producing a ferroelectric state in a magnetically ordered state, amongst stereochemical lone pair Bi^{3+} or Pb^{2+} based perovskites with magnetic transition-metal ions on the B-site, transverse-spiral (cycloidal) spin order breaking, geometrically driven distortions, charge ordering and electronic ferroelectricity on a specific chemical lattice are emphasized and multiferroicity has been revealed in the perovskite-type $BiFeO_3$ and $BiMnO_3$, orthorhombic $TbMnO_3$ and $TbMn_2O_5$, hexagonal $YMnO_3$, and spinel $LuFe_2O_4$[8–11].

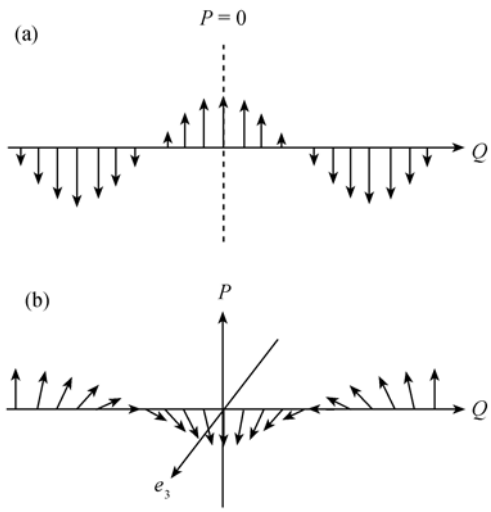

Figure 2 The sinusoidal SDW (a) does not induce a uniform electric polarization; for a helicoidal SDW (b) ***P*** is orthogonal both to the spin rotation axis e_3 and the wave vector ***Q***[16].

One of the most important ways known to now to produce ferroelectricity is the induction of spontaneous polarization in the spiral magnets by magnetic field. In the frustrated spin manganites of $RMnO_3$, RMn_2O_5, (R=Gd, Tb, Dy) and $Ni_3V_2O_8$[12–16], control of the spontaneous ferroelectric polarization with an external magnetic field has been demonstrated experimentally and theoretically. For instance, $TbMnO_3$ is in a large orthorhombic distorted structure with space group of *Pbnm* and regarded as a frustrated spin system having ferromagnetic nearest-neighbor and antiferromagnetic (AF) next-nearest-neighbor (NNN) interactions within a MnO_2 plane below Néel temperature of 41 K. The staggered orbital order associated with the $GdFeO_3$-type distortion induces the anisotropic NNN interaction, and yields unique sinusoidal and up-up-down-down AF ordered states in the distorted perovskites with e_g^1 configuration. Under magnetic field, this spin structure is broken and ferroelectric ordering established below 28 K, as schematically illustrated in the Figure 2. Using neutron diffraction, it was revealed that the spin structure is incommensurate and longitudinally modulated in the paraelectric phase, but there exists a transverse incommensurate spiral in the ferroelectric phase. It is suggested this spiral that breaks spatial inversion symmetry and induces magnetoelectricity in $TbMnO_3$. The spin helicity, clockwise or counterclockwise, is controlled by the direction of spontaneous polarization, which could be predicted in term of the ordering of Mn-O-Mn bond angles, and thus controlled by the polarity of the small electric field applied on cooling[16–18]. The disclosure of magnetic field induced spiral magnetoelectricity is very encourageous, nevertheless the extensive studies reveal that it is available only below 50 K[14,19].

In those conventionally practical proper ferroelectrics, there usually contains ferroelectric active cation without electrons filling on the *d* orbitals such as Ti^{4+}, Zr^{4+}, Nb^{5+} and Ta^{5+}. It was revealed theoretically by Cohen[20,21] and demonstrated experimentally by Kuroiwa et al.[22] that the hybridization between B-site ion d^0 and O $2p^6$ plays a dominant role for the instability of ferroelectricity, and that the spontaneous ferroelastic distortion and the hybridization between A-site ion and O could further enhance the ferroelectric polarization and ordering temperature. On the other hand, the ferroelectric- paraelectric phase transition has been often discussed from two limiting cases: the soft-mode or displacive theory, in which a transverse optical mode gradually softens when approaching the phase transition, and an order-disorder scenario, in which some atoms lying on symmetry-equivalent sites occupy on some preferential ones. High pressure XAFS and X-ray diffuse scattering measurements can give a unique opportunity to disentangle the role of the lattice dynamics and the local order of the B atoms in the ferroelectric phases of perovskites. Recent observations of the diffuse lines in the high-pressure cubic phase of $BaTiO_3$ and their intensities decreasing linearly to zero at ~11 GPa demonstrates that the B atom disorder enhances the ferroelectric instability and is an essential ingredient for the stabilization of the ferroelectric state[23]. Therefore, current theory of an intermediate situation, in which both soft phonons and disorder play a role, is being preferred and developed. Nevertheless, the present understanding on the mechanism of origin of ferroelectricity and their controlling factors is still on the qualitative level but not quatitative.

From an experimental viewpoint, it was observed that in general the transition metal *d* electrons, essential for magnetism, reduce the tendency for off-center ferroelectric distortion. This fact has been discussed theoretically in details by Hill and termed as *exclusion rule* for the simple perovskite crystal structure, of which both ferromagnetism requiring d^n configuration and ferroelectricity favoured by d^0 configuration rely on the same cationic sublattice and cannot be fulfilled simultane-

ously[24]. This very significant drawback drives one to search alternative electrical or structural driving force for ferromagnetism and ferroelectricity to occur simultaneously in the possible single-phased multiferroic materials. Under hints by the case of $BiFeO_3$, which seems to violate the d^0 requirement for ferroelectricity, Spaldin and her coworkers proposed the stereochemical activity of Bi^{3+} lone pair on the A-site as driving force for ferroelectricity and the B-site ions of such as Mn^{3+} and Cr^{3+} for magnetism, and demonstrated through *ab initio* calculations that $BiMnO_3$ and $BiCrO_3$ are possible multiferroics[24–26]. Then, a series of metastable perovskite-type $BiMnO_3$, $BiCrO_3$, $BiCoO_3$, $BiNiO_3$, $PbVO_3$, Bi_2CrFeO_6, $BiMnO_3$-$BiCrO_3$, $BiCrO_3$-$BiFeO_3$ solid solutions have been attempted to synthesize under high pressure and check experimentally[27–30].

In the following sections, with examples of $BiFeO_3$, $BiMnO_3$ and Bi_2FeCrO_6, the difficulties encountered in this field are analyzed in details.

2 Bismuth ferrite

$BiFeO_3$ is well known to be the only prototypical material that possesses both high ferroelectric Curie temperature T_C = 1143 K and high antiferromagnetic Néel temperature T_N = 643 K[31]. Structurally, $BiFeO_3$ crystallizes in a rhombohedrally distorted perovskite structure with *R3c* space group at room temperature, of which the lattice constants were determined as a_H = 5.587 Å, c_H = 13.867 Å in the hexagonal unit cell containing six formula or a_R = 5.638 Å, β = 59.348° in the rhombohedral unit cell containing two formula units[31–33]. Three main distortions are responsible for the existence of spontaneous polarization along the $[001]_{hex}$ direction (i.e. $[111]_{cub}$): the oxygen octahedra are rotated by about $\pm\alpha$=13.8° around the 3-fold axis and distorted with minimum and maximum O-O distances of 2.71 and 3.02 Å, respectively, bismuth and iron atoms are shifted by 0.54 and 0.13 Å, respectively, along the 3-fold axis[33]. These structural data implies that $BiFeO_3$ is a ferroelectric compound with a G-type-like antiferromagnetism.

2.1 Synthesis

The synthesis of pure $BiFeO_3$ samples is quite subtle because it is necessary to take both kinetic and thermodynamic properties into account. As shown in the phase diagram of Bi_2O_3-Fe_2O_3 by Figure 3, two impurities of $Bi_{25}FeO_{39}$ and $Bi_2Fe_4O_9$ can be formed along with

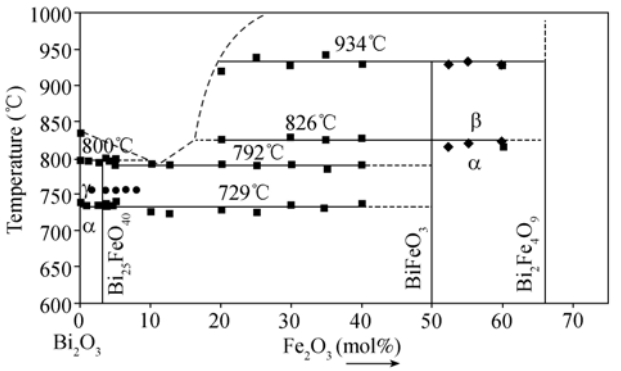

Figure 3 Phase diagram of Bi_2O_3-Fe_2O_3 in the temperature range 600−1000℃. Equilibria (●) were characterized after long annealing. Invariant temperatures (■) were determined by DSC runs. Allotropic transitions (♦) were studied by HTXRD and DSC[34].

perovskite-structured $BiFeO_3$[34,35]. The high volatility of Bi_2O_3 leads to formation of Bi-poor phase $Bi_2Fe_4O_9$, but a small excess of Bi_2O_3 in the reactants, necessary to compensate for the loss of Bi_2O_3, leads to formation of Bi-rich phase $Bi_{25}FeO_{39}$. Differential thermal analysis and kinetic investigations show that the reaction in equimolar mixture of $BiFeO_3$ is complex: the reaction is incomplete below 675℃, but $BiFeO_3$ decomposes very slowly into $Bi_2Fe_4O_9$ when the temperature increases above 675 ℃ and rapidly into $Bi_2Fe_4O_9$ above 830℃[36–38]. To prevent the formation of $Bi_2Fe_4O_9$, the initially attempted synthesis of $BiFeO_3$ using solid state reactions and the growth of single crystal using flux method made use of a very large excess of Bi_2O_3 (100%), but the disadvantage of this technique is to form a large quantity of $Bi_{25}FeO_{39}$ that cannot be separated from $BiFeO_3$ with a good yield, even through leaching by diluted nitric acid[39,40]. In the form of both ceramics and single crystal of $BiFeO_3$, the presence of paramagnetic $Bi_{25}FeO_{39}$ or $Bi_{12}FeO_{19.5}$-Bi_2O_3 solid solution in sillenite structure and antiferromagnetic $Bi_2Fe_4O_9$ in the orthorhombic structure with T_N = 260 K have been demonstrated by the measurements of both X-ray diffraction and temperature-dependent magnetization, as illustrated by Figures 4 and 5[41–49].

2.2 Ceramics

As discussed above, the kinetic and thermodynamic properties of the Bi_2O_3-Fe_2O_3 system result in a very narrow sintering window to obtain very pure single phase of $BiFeO_3$. A rapid liquid-phase sintering technique has been developed by Liu group and widely used to synthesize highly pure single-phased $BiFeO_3$ ceram-

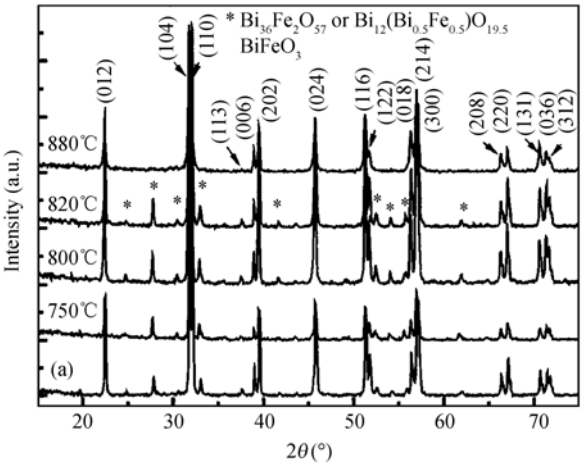

Figure 4 X-ray diffraction patterns of the $BiFeO_3$ ceramic samples synthesized by the rapid sintering processing at different sintering temperatures. Pure phase $BiFeO_3$ with high resistivity was synthesized at 880℃. Curve (a) shows the XRD pattern of $BiFeO_3$ ceramic sintered at 880℃ for 3 h by conventional solid state reaction sintering technique[41].

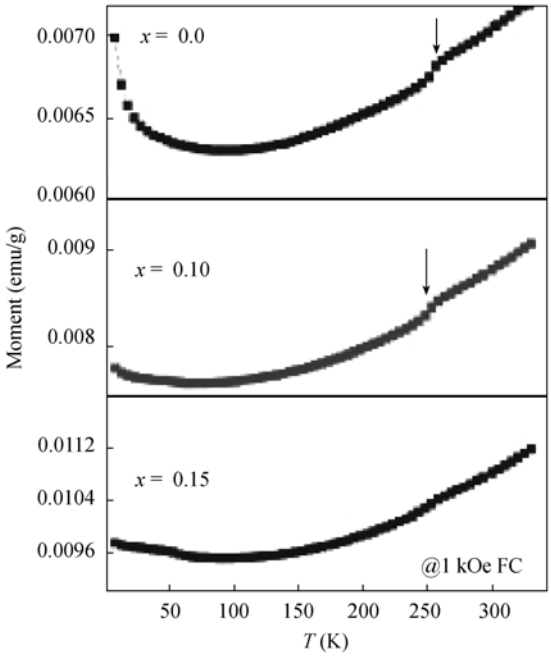

Figure 5 Temperature-dependent field cooling magnetizations of $Bi_{1-x}La_xFeO_3$ ceramics[42].

ics[41,48–50]. The as-prepared ceramic pellets could exhibit a high resistivity of the order of 6.7×10^{10} Ω·cm under an external electric field of 100 kV/cm, and saturated ferroelectric hysteresis loops were observed at room temperature with spontaneous polarization P_s = 8.9 μC/cm^2, remanent polarization P_r = 4.0 μC/cm^2, and coercive field E_c = 39 kV/cm under an applied field of 100 kV/cm for the sample sintered at 880℃ for 450 s[41], P_r = 11.7 μC/cm^2 under 155 kV/cm at 860℃ for 60 min[50]. Combining with the measurements of X-ray photoelectron spectroscopy analysis of oxygen, it was argued that the formation of Fe^{2+} and an oxygen deficiency leading to higher leakage current can be greatly suppressed by the very high heating rate, short sintering period, and liquid phase sintering technique. In contrast, for the $BiFeO_3$ ceramics synthesized under high pressure, P_r = 46 μC/cm^2 and E_c = 73 kV/cm were obtained under an applied field of 120 kV/cm[51].

2.3 Leakage problem

From an experimental point of view, the characterization of ferroelectric behavior of $BiFeO_3$ at room temperature has proven to be a very difficult task, which comes from the high conductivity of $BiFeO_3$ at temperatures above 190 K, preventing the application of high electric field and substantially making confused those characterizations of magnetic and electrical properties[52]. Recently, more detailed analysis of experimental measurements of electric field dependence of leakage current density (J-E) for the $BiFeO_3$ and related ceramics and thin films reveal that J increases linearly with low electric field, elucidating an ohmic conduction mechanism in this region, while the most probable conduction mechanism for high electric field region seems extrinsic due to the thermal excitation of inner charged defects, described by the conduction mechanisms of space-charge-limited current characterized by the linear relationship of J-E^2[53,54], Schottky by $\ln J$-$E^{1/2}$[55,56] and/or Poole-Frenkel by $\ln(J/E)$-$E^{1/2}$[45,57–59]. On the other hand, the band structure of $BiFeO_3$ was calculated to be indirect with band gap of 2.8 eV by the density-functional based screened exchange method[60] and determined as direct 2.36 eV through transmission spectroscopy measurements of $BiFeO_3$ films on fused silica[61] and 2.5 eV in the single crystal sample[35], which is much smaller than 3.2 eV of $BaTiO_3$[62].

In the epitaxial c-axis oriented $BiFeO_3$ thin films on the $SrRuO_3/SrTiO_3$ (001) substrates, space-charge-limited current was found as the dominant leakage mechanism for both negative and positive biases at temperatures between 80 and 150 K, but at temperatures between 200 and 350 K the dominant mechanisms were Poole-Frenkle emission and Fowler-Nordheim tunneling for negative and positive biases, respectively[53]. For the $BiFeO_3$ thin films, doping of 2 at% Ti^{4+} ions was experimentally found to increase the dc resistivity by more than three orders of magnitude but doping of Ni^{2+} to

reduce the dc resistivity by two orders of magnitude. At room temperature under 10 kV/cm applied field, the resistivity was measured typical of 5.8×10^6, 9.5×10^8 and 1.5×10^{11} Ω·cm for Ni^{2+}-doped, pure and Ti^{4+}-doped films, respectively. Current-voltage characteristics indicated that the main conduction mechanism for pure and Ni^{2+} doped thin films was space charge limited, which was associated with the free-carriers trapped by the oxygen vacancies, whereas in the Ti^{4+} doped films, field-assisted ionic conduction was dominant[63,64]. In the $BiFeO_3$ ceramics, Nb- or Ti-doping was found efficient to increase the electrical resistivity by about 6 orders of magnitude and the activation energy enhanced by Nb-doping from 0.58 (0%) to 1.11(3%) eV[65,66].

For $BiFeO_3$, codoping technique has been demonstrated experimentally more effective to improve the insulating property. By codoping La and Ni atoms in the $BiFeO_3$ thin films formed by chemical solution deposition on Pt/Ti/SiO_2/Si (100) substrate, as illustrated in Figures 6 and 7, the leakage current density was reduced lower than 1×10^{-3} A/cm^2 at 500 kV/cm while well saturated loop with P_r = 70 μC/cm^2 was obtained at room temperature and frequency 10 kHz[67]. Adding 5 mol% $LaMnO_3$ into $BiFeO_3$ thin film, P_r = 45 μC/cm^2 and E_c = 215 kV/cm was obtained at room temperature and 1 kHz[68]. For the 5 mol% Pb- and 3 mol% Cr-cosubstituted $BiFeO_3$ film, P_r = 62 μC/cm^2 and E_c = 235 kV/cm were obtained at room temperature under applied field of 712 kV/cm[69].

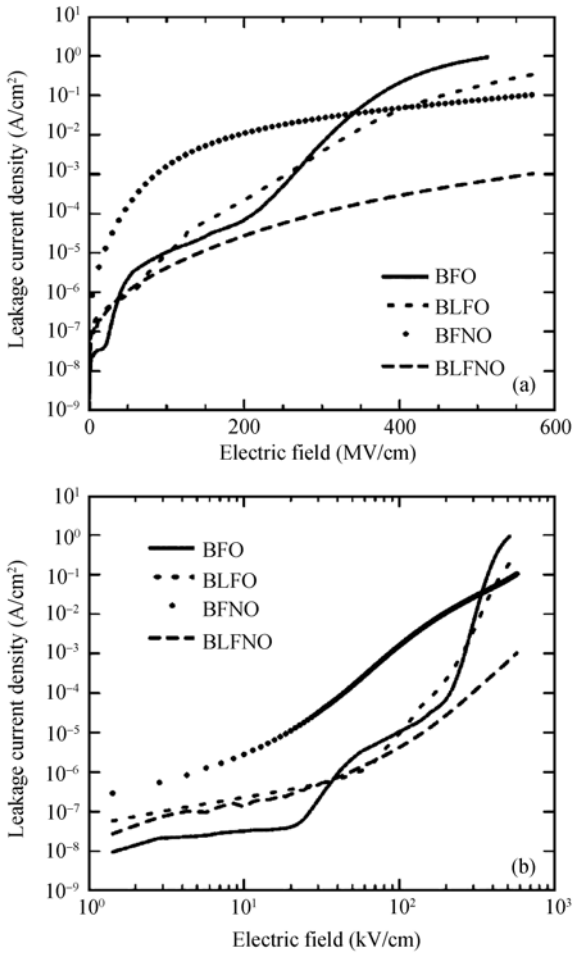

Figure 6 *J-E* characteristics of pure, 5 at% La-doped, 5 at% Ni-doped, 2.5 at% La- and Ni-codoped $BiFeO_3$ films on the Pt/Ti/SiO_2/Si(100) substrate measured at room temperature[67]. (a) Semilogarithmic; (b) logarithmic plots.

2.4 Single crystal

Shortly after its discovery, $BiFeO_3$ single crystals were initially grown by a flux method with Bi_2O_3 or Bi_2O_3/B_2O_3/Fe_2O_3 as flux[70,71]. Recently, highly pure $BiFeO_3$ single crystals were grown by a spontaneous crystallization in air from a Bi_2O_3-Fe_2O_3 flux[40,72]. It was demonstrated that $BiFeO_3$ is indeed ferroelectric at room temperature through evidences measured by electric polarization vs. field hysteresis loops and piezoresponse force microscopy. For the sample with high resistivity of 6×10^{10} Ω·cm at room temperature under 100 V, a large spontaneous polarization was observed with remanent polarization $P_{[012]}$=60 μC/cm^2 and E_c =12 kV/cm, which is presented in Figure 8. Inferred from the first polarization loop, a large intrinsic saturation polarization along the $[001]_{hex}$ direction is close to 100 μC/cm^2, agreed well with theoretical prediction of 90—100 μC/cm^2 using density functional theory[73]. Measurements of several successive polarization loops showed that the samples become gradually harder to polarize as coercive and saturation fields increase and remanent polarization decreases with cycling, eventually reaching fields where leakage currents prevent the application of a large enough voltage. With an optical microscopy, *in-situ* observations confirmed microcracks induced by mechanical stresses owing to piezoelectric effect during reversal, which prevents domain walls moving easily through the sample.

2.5 Magnetic structure

For $BiFeO_3$, the Fe^{3+} ions on the B-site were determined by neutron diffraction as antiferromagnetically ordering with magnetic moment of μ_{Fe} = 3.70 μ_B[74,75]. Moreover, it was found that the high resolution neutron powder

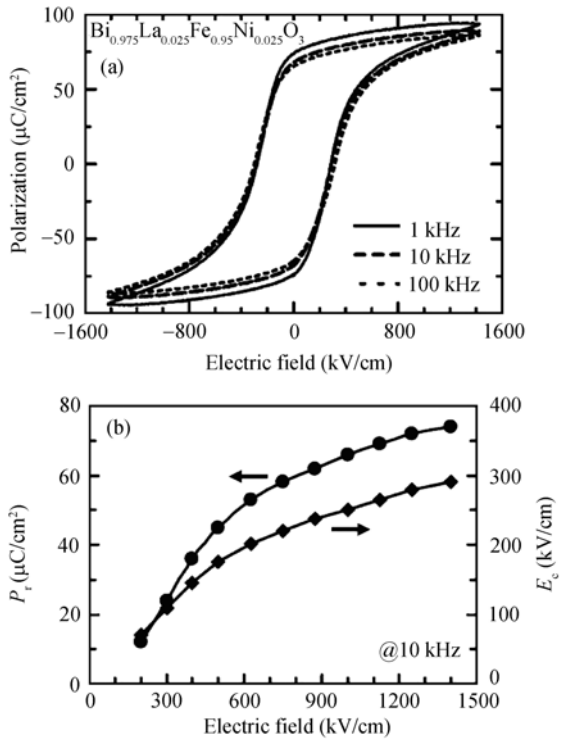

Figure 7 (a) *P-E* hysteresis loops of a 2.5 at% La- and Ni-codoped $BiFeO_3$ film capacitor measured at 1, 10 and 100 kHz; (b) applied electric field dependences of the remanent polarization (P_r) and coercive field (E_c) measured at 10 kHz[67].

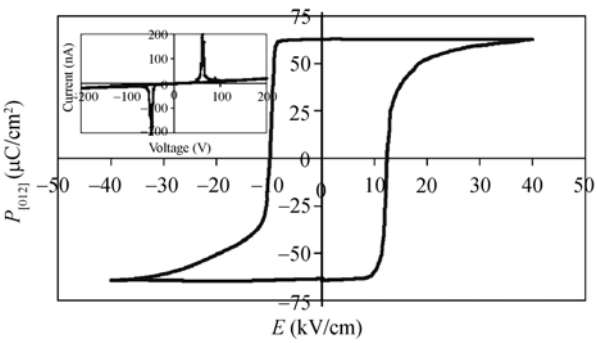

Figure 8 The first full *P-E* hysteresis loop of the $BiFeO_3$ single crystal at room temperature. The remanent polarization $P_{[012]}$ is 60 μC/cm^2 and the coercive field is 12 kV/cm. The inferred full saturation polarization along the $[001]_{hex}$ direction is close to 100 μC/cm^2. Insert, Raw I(V) data[72].

diffraction patterns of $BiFeO_3$ could be described with the same accuracy by several modulated magnetic ordering models: circular cycloid, elliptical cycloid and spin density wave[76]. In contrast to the recent models for the magnetoelectric coupling observed in $TbMnO_3$ perovskites[16,77,78], to clarify this ambiguity of the magnetic ordering in $BiFeO_3$ is very important. Through analysis of zero-field NMR spectrum lineshape of the ^{57}Fe-enriched $BiFeO_3$[79,80], a long-range spatially modulated, incommensurate cycloidal spin structure was discriminated as schematically presented in Figure 9 and the antiferromagnetically ordered spins rotate onto the plane containing the threefold axis of rhombohedral unit cell, of which the wave vector is along the [110] direction and lies in the plane of spin-rotation $(1\bar{1}0)$, and the period λ = 620 Å being incommensurate to the lattice spacing. This complex spin structure found in $BiFeO_3$ can be interpreted in terms of relativistic Lifshitz invariants and described by the equation

$$\cos\theta(x) = sn\left(\pm\frac{4K(m)}{\lambda}x, m\right),$$

where θ is the angle of spin rotation relative to the *c* axis, *x* is the coordinate along the cycloid propagation direction, $sn(x, m)$ is the Jacobian elliptic function, *m* is its parameter, and $K(m)$ is a complete elliptic integral of the first kind[81,82].

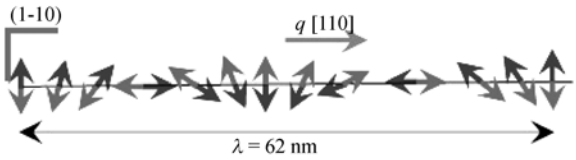

Figure 9 Schematic antiferromagnetic structure of $BiFeO_3$ where the two antiferromagnetic sublattices are organized along a cycloidal spiral. The propagation vector $\boldsymbol{q}$ is along the direction [110] and the plane of spin-rotation is $(1\bar{1}0)$ [40].

Owing to the presence of spin cycloidal magnetic structure, the field and temperature dependent magnetization measurements should be and have been observed to exhibit a pure antiferromagnetic response, without any trace of weak ferromagnetism, in the pure $BiFeO_3$ single crystals[40,83]. This behavior is further confirmed by the line broadenings of the Mössbauer spectra, due to the slight modulation of the hyperfine energies as the magnetic moment rotates with respect to the principal axis of the electric field gradient tensor. Therefore, it is of interest to note that weak ferromagnetism often reported in the polycrystalline $BiFeO_3$ ceramics and thin films is in fact mostly due to the presence of a small amount of magnetic impurity, even though it is now generally accepted that the observed spontaneous magnetization in the as-prepared $BiFeO_3$ samples is a cumulative effect of mixed Fe^{2+}/Fe^{3+} valence formation, suppression of inhomogeneous spin structure, an increase in canting angle, and/or iron-rich nanoclusters[50,59,84–88]. For instance, the spin-glass behaviors were observed in the *M-T* and *M-H* measurements for the $BiFeO_3$ films

annealed in the air atmosphere, and further enhanced by annealing the sample in the oxygen atmosphere, which supports the fact of the formation of iron oxide nanoclusters or precipitates[87,88]. To clarify this anomalous ferromagnetism observed in those as-prepared samples, it is necessary to extensively conduct measurements of transmission electron microscopy and X-ray photoemission spectroscopy to remove the effects of magnetic impurities and NMR to confirm breaking of the spin cycloidal magnetic structure.

2.6 Magnetoelectric effect

In the $BiFeO_3$, the presence of spin cycloidal modulation magnetic structure forbids the first-order magnetoelectric coupling effect and shows the quadratic effect. Using the quadratic magnetoelectric effect, the components of the nonlinear magnetoelectric susceptibility tensor β_{ijk} were determined at 4 K as $\beta_{111} = 5.0\times10^{-19}$, $\beta_{113} = 8.1\times10^{-19}$, $\beta_{311} = 0.3\times10^{-19}$, $\beta_{333} = 2.1\times10^{-19}$ s/A[89]. Under a pulsed field up to 280 kOe at $T = 10-180$ K, electric polarization components were measured with the help of electrodes attached to the faces of single crystal. As presented in Figure 10, the measured dependence of $P(H)$ is quadratic at $H < H_c$ and has a jump at $H = H_c$ when the spin cycloidal structure is evidently destroyed. The critical field H_c is of the order 200 kOe[90,91]. So far, it has been shown that the destruction of such cycloidal structure in the $BiFeO_3$ by a high magnetic field leads to the onset of linear magnetoelectric effect and the appearance of a toroidal moment, based on the experimental observation that the off-diagonal components of the linear ME effect tensor are asymmetric ($\alpha_{12} = -\alpha_{21}$ for $\boldsymbol{L} \parallel c$, where $\boldsymbol{L}$ is the antiferromagnetic vector).

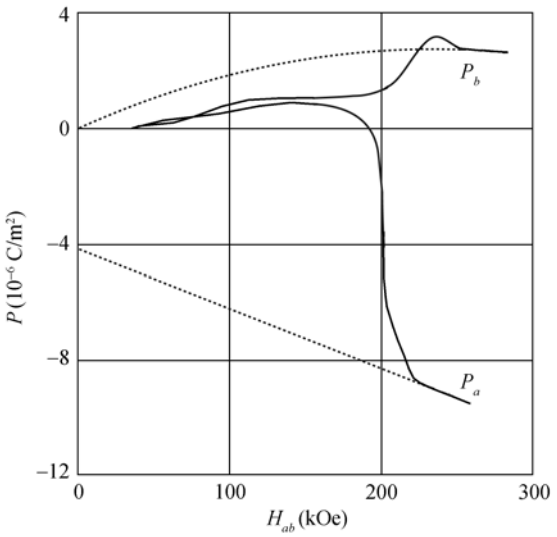

Figure 10 Experimental curves of the components of the electric polarization of $BiFeO_3$ along the a and b axis (P_a and P_b) at a temperature of 20 K as functions of the magnetic field applied in the basal plane at a 45° angle to the a axis. The dashed lines show the straight line and parabola which approximate the experimental curves in the region H>250 kOe[91].

In addition to high magnetic field[91–94], the composition modification of randomly distributed charged imperfections at A-site or/and B-site[43,95–99] and expitaxial strain[83,84] have also been proposed to induce such phase transition from the incommensurate cycloidal spin state into the homogeneous antiferromagnetic state and release the latent magnetization and linear magnetoelectric effect of $BiFeO_3$, to make $BiFeO_3$-based materials efficient room-temperature single-phased magnetoelectric multiferroics. Substituting Bi with rare earth, the quadratic magnetoelectric effect was found in the rhombohedral and triclinic phases, and the linear magnetoelectric effect was observed in the orthorhombic structure, the magnitude of which depends on the nature of the rare-earth element[100]. With $LaFeO_3$ of symmetry *Pnma* and uniform magnetic structure, the spin cycloidal magnetic structure has been demonstrated to destroy into an ordinary spatially uniform antiferromagnetic state near the concentration of 20%, corresponding to the phase transition with a change in the unit-cell symmetry *R3c* to *C222*[44,99]. In the $(Bi_{1-x}La_x)FeO_3$ solid solutions, the Curie temperature decreases linearly with increasing La concentration, e.g. from 820℃ for $x = 0.0$ to ~405℃ for $x = 0.3$. For $0\leqslant x\leqslant 0.75$, the solid solutions are ferroelectric while they are antiferromagnetic at $0\leqslant x\leqslant 0.20$ and become weak parasitic ferromagnetic at $x\geqslant 0.20$[101].

By the end of this section, it is of interest to note that, through measurements of infrared reflectivity and time domain terahertz transmission spectroscopy at temperature of 20—950 K and the magnetodielectric effect at 10—300 K with the magnetic field up to 9 T, the magnetodielectric effect observed below 175 K in the $BiFeO_3$ ceramics was found lower by several orders of magnitude due to the decreased conductivity and agreed well with contributions of sum of polar phonons, while a giant low-frequency permittivity observed at higher temperatures obviously due to the enhanced conductivity and Maxwell-Wagner contribution[102,103].

3 Bismuth manganite

$BiMnO_3$ is to be potential ferromagnetic-ferroelectric

multiferroic proposed theoretically by Hill and Rabe[104] and experimentally demonstrated by Sugawara et al.[105,106] and Kimura et al.[107]. In general, the perovskite-structured $BiMnO_3$ was synthesized in a rather wide temperature range (600—900℃) and a relatively narrow pressures of 40—50 kbar. A deviation from these conditions results in the disappearance of the perovskite phase[27]. It is determined by X-ray diffraction, electron diffraction and neutron powder diffraction as a heavily distorted perovskite structure, having monoclinic symmetry with a noncentrosymmetric $C2$ space group and lattice parameters of a = 9.5323 Å, b = 5.6064 Å, c = 9.8535 Å, and β = 110.667°. The noncentrosymmetrical distortion is revealed below ~750−770 K and caused by a polarized Bi $6s^2$ lone pair. However, it is difficult to observe its ferroelectricity directly in the conventionally experimental polarization measurements due to high leakage current. In the $BiMnO_3$ epitaxial films, the ferroelectricity was demonstrated by optical second-harmonic generation (SHG), of which the change in the polar symmetry of SHG signals under external electric field is correlated to specific changes in the ferroelectric domain microstructures and effective d_{eff} ~193 pm/V under electric fields of 707 V/mm obtained[108]. Nevertheless, recent structural characterizations on polycrystalline $BiMnO_3$ samples revealed that the actual structure depends sensitively on the oxygen stoichiometry and is in the centrosymmetric $C2/c$ space group[109−111].

The measurements of temperature dependent magnetization and specific heat revealed the onset of ferromagnetic ordering at ~105 K, with the second order nature. Careful examination of the six unique Mn-O-Mn superexchange pathways between the three crystallographically independent Mn^{3+} sites shows that four are ferromagnetic and two are antiferromagnetic, confirming that the ferromagnetism of $BiMnO_3$ stems directly from orbital ordering, with a collinear ferromagnetic structure having spin direction along [010] and magnetic moment of 3.2 μ_B. Every trivalent manganese cation exhibits the Jahn-Teller distortion and ordering of a vacant $d_{x^2-y^2}$ orbital is suggested to play an important role for the ferromagnetism[112,113].

On cooling the polar room-temperature structure to 20 K, there is no crystallographic phase transition, implying that ferromagnetism and ferroelectricity coexist in $BiMnO_3$. In the measurements of temperature dependent dielectric constant, a fairly large negative magnetocapacitance effect was observed in the vicinity of the ferromagnetic transition temperature T_C, which is well described as $-\Delta\varepsilon/\varepsilon(0) = kM^2$. This magnetocapacitance effect could be phenomenologically interpreted in terms of a simple Landau-Ginzburg theory for the second-order phase transition of ferroelectromagnets, which is ascribed to the magnetoelectric coupling term γP^2M^2 in the thermodynamic potential[107].

4 Bismuth chromate ferrite

In the cases of perovskite $BiMO_3$ (M = Fe, Mn, Cr, Co, Ni), the B-site is occupied by the same transition metal element and usually antiferromagnetic ordering prevails, except for $BiMnO_3$ with predominant orbital ferromagnetic ordering. According to Goodenough-Kanamori rule, the spin coupling through Fe d^5-O-Cr d^3 bond would produce ferromagnetic ordering in the ordered double perovskite. With stereochemically active Bi $6s^2$ lone pair as driving force for ferroelectricity, the ordered double perovskite Bi_2FeCrO_6 was proposed to be possible high temperature ferromagnetic-ferroelectric multiferroic compound. Spaldin et al. calculated the magnetic structure and ferroelectric polarization in the ordered Bi_2FeCrO_6 using first-principle density functional theory under LDA+U approximation[26,114]. In comparison with the cases of $BiCrO_3$ and $BiFeO_3$, it was revealed that the on-site Coulomb repulsion in Bi_2FeCrO_6 is the main force for the stabilization of high-spin state of Fe^{3+} cation, which results in increasing volume and lattice constants but reducing rhombohedral angle over the series of $BiCrO_3$, Bi_2FeCrO_6, $BiFeO_3$, due to the larger radius of the high-spin Fe^{3+} ion compared with that of Cr^{3+}. The calculated density of states indicates that both the top of the valence band and the bottom of the conduction band are 100% spin polarized, with electrons confined to narrow, up-spin Fe $3d$ bands, and holes in broader, up-spin Cr $3d$-O$2p$ hybrids. It is a little surprising that the magnetic nearest-neighbor coupling constants was demonstrated to be negative for Bi_2FeCrO_6 with low-symmetry space groups and the ground state is the G-type-like antiferromagnetic configuration with magnetic moment of 2 μ_B per formula unit. Under a mean-field approximation, the magnetic ordering temperature would not exceed 100 K for the ground-state structure. Moreover, a spontaneous polarization of 79.6

μC/cm^2 was predicted for the ground state with space group of $R3$.

Basically, such a predicted double perovskite compound with long range B-site cation order is not likely to form since Fe^{3+} (r = 0.645 Å) and Cr^{3+} (r = 0.615 Å) have the same charge and close ionic sizes. Metastable $Bi(Fe_{1/2}Cr_{1/2})O_3$ is expected to adopt a simple perovskite structure with random occupancy of Fe^{3+} and Cr^{3+} on the B-site. Recent experimental works confirmed that the $Bi(Fe_{1/2}Cr_{1/2})O_3$ in the form of bulk ceramics and epitaxial thin film is isostructural to $BiFeO_3$ with a rhombohedral distortion. Suchomel et al. attempted to prepare perovskite-structured $Bi(Fe_{1/2}Cr_{1/2})O_3$ ceramics by high pressure solid-state synthesis at a pressure of 6 GPa and 1000℃[115]. They found that it was isostructural to polar $BiFeO_3$, in a hexagonal $R3c$ unit-cell structure with lattice parameters of a = 5.545 Å and c = 13.695 Å and stable up to 400℃ at ambient pressure, above which it decomposes to $BiFeO_3$ and other phases. The Bi and mixed Fe/Cr B-site cations are displaced from their ideal positions along the threefold symmetric direction by 0.58 and 0.22 Å, respectively. These displacements give rise to a static polarization of 63 μC/cm^2, calculated using the ionic charge model, along the hexagonal [001] direction. Bond valence sum calculations for the refined perovskite structure at room temperature give valences of +2.95, +3.10, +2.82, and –1.97 for the Bi^{3+}, Fe^{3+}, Cr^{3+}, and O^{2-} ion sites, respectively. The slight overbonding and underbonding of Fe^{3+} and Cr^{3+} are consistent with the difference in ionic radii of these two cation species. Owing to the disorder of Fe^{3+} and Cr^{3+} cations on the B-site in the present samples, Mössbauer and magnetization measurements showed that the intrinsic magnetism is dominated by antiferromagnetic exchange interaction and exhibits spin glass-like freezing below 130 K.

According to the structural parameters obtained by Suchomel et al.[115], the equivalent pseudocubic lattice parameters in a rhombohedral unit cell are a = 3.932 Å and β = 89.7°. With a small in-plane lattice mismatch of 0.7% and a likely rhombohedral tilt, it is expected a pseudomorphic growth of films on the $SrTiO_3$ (001) substrate up to 300 nm thickness to stabilize metastable $Bi(Fe_{1/2}Cr_{1/2})O_3$[116–118]. For the epitaxial $Bi(Fe_{1/2}Cr_{1/2})O_3$ thin films, a tetragonal-like structure was experimentally revealed with lattice constants of $a = b$ = 3.905 Å in plane and c = 3.965 Å out of plane. The electrical measurements observed a ferroelectricity with dielectric polarization of 2.8 μC/cm^2 at E_{max} = 82 kV/cm for one 300 nm thick film at room temperature[116], 60 μC/cm^2 along the pseudocubic [001] direction at 77.3 K[117]. However, similar to the case of $BiFeO_3$, these measurements of electric and magnetic properties are also confused by the parasitic impurity phases and high leakage current of the as-prepared samples.

With respect to Bi_2FeCrO_6 compound, even though some attempts have been performed to grow it in the form of thin film and bulk ceramics, which showed disordered and not pure samples, it is still a big challenge to develop proper preparation method to obtain metastable B-site ordered perovskite-structured Bi_2FeCrO_6. Recent experiments conducted by one of the authors indicate that R-type ferrimagnetic ordering with Curie temperature higher than room temperature can be expected if the chemical ordering between Fe and Cr on the B site is increased[119,120].

5 Relationship between magnetic structure and crystal symmetry

5.1 Superexchange theory

According to Anderson[121], the superexchange interaction in perovskite-type oxides can be separated into two contributions: (i) kinetic exchange which is due to the mixing of the ligand-field orbitals used to describe the spin quasiparticles; this term is proportional to b^2/U and is always antiferromagnetic, and (ii) potential exchange which represents the direct exchange interaction between these ligand-field orbitals; this term is always ferromagnetic. Based on this separation, the following simple guidelines for estimating the sign and relative magnitude of superexchange interactions are obtained, with the same outcomes as from the Goodenough-Kanamori rules[26]:

(i) Usually, the kinetic exchange is much stronger than the potential exchange and dominates, leading to the predominantly antiferromagnetic interactions.

(ii) The kinetic exchange between e_g electrons on different ions connected by a 180° metal-oxygen-metal bond is much stronger than that between corresponding t_{2g} electrons, since the former is mediated by $dp\sigma$ bonds whereas the latter by weaker $dp\pi$ interactions.

(iii) In certain situations the kinetic exchange vanishes by symmetry so that the remaining potential exchange leads to a small ferromagnetic coupling. This occurs for example for a 90° superexchange coupling

between t_{2g} electrons and also in the case of a 180° coupling between e_g and t_{2g} electrons.

(iv) Completely filled manifolds with equal numbers of up- and down-spin electrons give no net contribution to the superexchange interaction.

5.2 Effect of lattice distortion

The Goodenough-Kanamori rules are derived on the basis of hypothesis of that the orbital occupation is static, and they work well in a wide range of the magnetism of correlated Mott insulators because a structural phase transition, driven by the Jahn-Teller coupling of degenerate orbitals to the lattice, lifts the degeneracy and fixes the orbital occupation well above the magnetic transition[122–124]. They stated that if there is large overlap between partly occupied orbitals at two magnetic ions, the superexchange interaction between them is strongly antiferromagnetic (AF) because of the Pauli principle, whereas overlap between partly occupied and unoccupied orbitals gives weakly ferromagnetic (FM) interaction due to Hunds exchange[120]. In the archetypical case of 180° bonds through a single ligand ion, this translates into a complementary interdependence between spin order and orbital order[125]: ferro-orbital (FO) order supports strong AF spin order, while alternating orbital (AO) order supports weak FM spin order. The canonical example of this behavior is $KCuF_3$, where weak FM (positive) spin correlations in the *ab* plane and strong AF (negative) correlations along the *c* axis are accompanied by AO order in the *ab* planes and FO order along the *c* axis. This happens typically for electrons in e_g orbitals where large Jahn-Teller distortions favor C-type orbital order, as in $KCuF_3$ and $BiMnO_3$.

The effect of lattice distortions on the magnetic behavior of perovskite-type manganites were ever extensively studied for the binary systems $Nd_{1-x}M_xMnO_3$, and the ternary systems $(Bi_{1-x}La_x)_{0.5}Ca_{0.5}MnO_3$ and $Bi_{0.5}(Ca_{1-x}M_x)_{0.5}MnO_3$, where M = Ca^{2+}, Sr^{2+}, Ba^{2+}, Pb^{2+}[126–128]. There exists a correlation between lattice distortions and magnetic behavior: (i) cubic and slightly distorted compounds exhibit a pure ferromagnetism; (ii) distortions from the cubic structure give reduced spontaneous moments and in some cases antiferromagnetism develops. That is to say, the ferromagnetic nature of the Mn^{3+}-O_2-Mn^{3+} and Mn^{3+}-O_2-Mn^{4+} interactions found in the nondistorted compounds is well agreed with the Goodenough rules. When the lattice becomes distorted away from cubic, the subtended angle in the Mn-O_2-Mn linkage decreases from 180°, this fact disturbs the orbital orthogonality and results in an increase of the antiferromagnetic t_{2g}-t_{2g} interaction via σ-bond and in the occurrence of other superexchange antiferromagnetic interactions which couple both the e_g and t_{2g} orbitals and the t_{2g} and t_{2g} orbitals via π-bond.

In the case of Bi_2FeCrO_6, although the ferromagnetic coupling is expected for the 180° $Cr^{3+}d^3$-O-Fe^{3+} d^5 bond from the Goodenough rule indicated in Figure 11, the antiferromagnetic coupling was illustrated to be stable ground state for the phases with lower symmetry than cubic. In the theoretical simulations of (111)-layer ordered Bi_2FeCrO_6 conducted by Spaldin et al.[26], it is found that the kinetic exchange between the e_g electrons of the Fe^{3+} and the t_{2g} electrons of the Cr^{3+} is drastically reduced and the net interaction becomes ferromagnetic in the cubic phase, whereas the nearest neighbor superexchange coupling between Fe^{3+} and Cr^{3+} becomes weakly antiferromagnetic in the relaxed structures with lower symmetry. It is the subtended Fe-O-Cr bond angle from 180°, which is caused by the off-center distortion necessary for ferroelectricity and/or octahedral rotation due to small tolerant factor, that enhances hybridization between Cr t_{2g} and Fe e_g states and thus leads to a nonzero kinetic exchange between these orbitals, resulting in antiferromagnetic coupling. This transformation between the ferromagnetic ordering in the paraelectric cubic phase and the ferrimagnetic one in the ferroelectric relaxed structure, predicted in term of Cr^{3+}-O-Fe^{3+} bond angle, could lead to one possible kind of magnetoelectric coupling effect when the ferroelectric-paraelectric Curie temperature is lower than magnetic ordering temperature. Such kind of materials is being under research by the authors.

5.3 Magnetic ordering temperature

In the 1960s, Goodenough investigated those predominant factors for Néel temperature in the perovskite structures and pointed out that a simple, localized-electron antiferromagnet having one electron per localized orbital interacting via 180° superexchange with similar orbitals on *z* near-neighbor cations via an overlap integral Δ has a Néel temperature:

$$kT_N \approx z\{q_t b_t^2 + q_e b_e^2\}(S+1)/S\,,$$

where q_t, q_e are inversely proportional to electrostatic energies associated with electron transfers; $b_t \sim \varepsilon_0 \Delta_t$ and $b_e \sim \varepsilon_0' \Delta_e$ are the one-electron transfer integral of states

Case	Outer-electron configuration	Correlation superexchange		Delocalization superexchange		Sum	Strength K (oxides)
		pσ	pπ	pσ	pπ		
#1	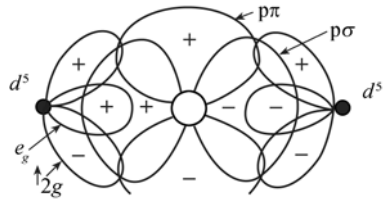	strong ↑↓	weak ↑↓	strong ↑↓	weak ↑↓	↑↓	~750
#2	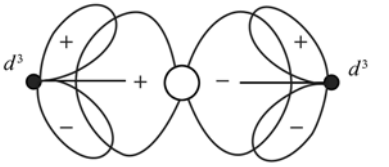	weak to moderate ↑↓	weak ↑↓	–	weak ↑↓	↑↓	$\lesssim$300
#3	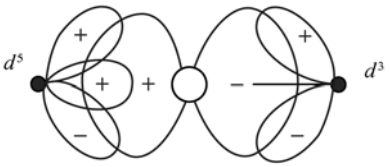	moderate ↑↑	weak ↑↓	moderate ↑↑	weak ↑↓	↑↑	~400

Figure 11 Three possible 180° cation-anion-cation interactions between octahedral-site cations. The pπ orbitals are not indicated in the diagrams for the cases 2 and 3[124].

having t_{2g} and e_g symmetry, respectively[129]. Accordingly, $dT_N/dp>0$, where p is the hydrostatic pressure and thus $dT_N/da_0>0$, where a_0 is the cation-anion-cation separation, remains in the localized d electron systems including $A^{3+}FeO_3$ and $A^{3+}CrO_3$. This fact is attributed to changes in A-O covalent bonding that cause Δ to increase with the more basic A cation for a given lattice parameter. For $BiFeO_3$ and $BiCrO_3$, the antiferromagnetic coupling between the e_g electrons on neighboring Fe sites due to the $dp\sigma$ bonding is very much stronger than that between the t_{2g} electrons on neighboring Cr sites, and thus results in $BiFeO_3$ having a higher magnetic ordering temperature than $BiCrO_3$. On the basis of the simulations for $BiCrO_3$, Bi_2FeCrO_6 and $BiFeO_3$, it was found that high magnetic ordering temperature can be achieved in the antiferromagnets or ferrimagnets by exploiting strong antiferromagnetic superexchange between e_g electrons. Therefore, it is reasonably expected to combine d^5 and d^8 ions for multiferroic compounds to obtain the highest magnetic ordering temperature in the perovskite structure[26].

6 Prospects for the future

From a practical point of view, it is very important and still a challenge to develop high temperature ferromagnetic-ferroelectric multiferroic single-phased compounds. Although several mechanisms for coexistence of magnetic and ferroelectric ordering have been disclosed and extensively studied[11], it is unclear how to get high temperature single-phased ferromagnetic-ferroelectric multiferroicity yet. For instance, the magnetic ordering temperature of rare earth manganites in both hexagonal and orthorhombic structures is below 139 K[14,19,130].

Perovskite transition-metal oxides form a unique category of multiferroic materials and could exhibit ferroelectricity, ferromagnetism and multiferroicity. Through theoretical calculations of electronic structures, the electron exchange interaction and correlation are responsible for the stabilization of electric polarization and the formation of magnetic moment, it has been revealed that the orbital hybridization (bonding) plays a central role in controlling ferroelectric and magnetic ordering[131]. For example, the antiferromagnetic superexchange is a result of energy lowering of occupied states due to its hybridization with the excited states, and the ferromagnetic double exchange comes from band broadening due to hybridization. The ferromagnetic double exchange mechanism is closely associated with metallic state with a positive temperature coefficient of resistivity while antiferromagnetic superexchange one associated with insulating state with a negative temperature coefficient of resistivity[132]. The effective charge associated with displacement of ions, which is

closely related to the dielectric polarization and known as Born effective charge, is significantly enhanced by the orbital hybridization (bonding), as the present widely accepted theory for ferroelectric instability. Therefore, it is possible through thorough investigations on the orbital hybridization behaviors in the perovskite-type transition metal oxides to balance the coexistence of ferromagnetic and ferroelectric ordering in single-phased compounds, and to obtain both high ordering temperatures above room temperature by controlling hybridization intensity through controlling geometrical arrangement of atoms[20,120,129].

For the multiple-orbital transition-metal ions, the hybridization depends not only on the geometrical arrangement of atoms but also on the mode of orbital occupation or orbital ordering. Like in Jahn-Teller effect of the first order to lift energy level degeneracy and the second order for off-center displacements, orbital ordering and the lattice distortion are strongly coupled. In this way, magnetism, orbital ordering and lattice distortion are closely correlated, therefore perovskite-type transition metal oxides serve as an important playground for demonstrating the spin-orbital-lattice coupling effects and to develop novel high temperature ferromagnetic-ferroelectric magnetoelectric single-phased compounds. The ferroelectric, multiferroic and magnetoelectric materials treated in the field of dielectrics have to be robust insulators, so that a high field can be applied to reorienting the spontaneous polarization without causing conductivity. In practice, most of ferromagnetic materials are metallic, but magnetic insulators tend to show antiferromagnetic coupling through superexchange interaction between the magnetic ions. In future, ferromagnetic insulators are particularly desired to develop for multiferroic materials. The experimental studies on $La_{1-x}Sr_xMnO_3$ imply this feasibility for us beyond double exchange mechanism[133]. Secondly, it is usually not able to synthesize perovskite-structured compounds under ambient pressure when the structure tolerance factor less than 0.96. Like in the cases of $BiFeO_3$, $BiMnO_3$ and $Bi(Fe_{1/2}Cr_{1/2})O_3$, it is difficult to obtain very pure single phase even with high-pressure synthesis. Thirdly, magnetic transition metal ions tend to be fairly easy to oxidize or reduce, and are usually associated with multiple valence states accompanied by anion nonstoichiometry. This fact increases the difficulties in synthesization and sintering process to obtain desired pure perovskite-type compounds. Therefore, it is important studying the conductivity mechanism to distinguish between intrinsic Mott metal-insulator phase transition and extrinsic leakage current owing to the defects and impurity phases, developing novel method to synthesize metastable perovskite-type compounds, and developing novel characterization method and setups to probe ferroelectric polarization and its switching, in particular for poor insulating samples.

1 Dzyaloshinskii I E. The magnetoelectric effect in antiferromagnetic materials. Sov Phys JETP, 1959, 10: 628
2 Astrov D N. The magnetoelectric effect in antiferromagnetic materials. Sov Phys JETP, 1960, 11: 708
3 Smolenskii G A, Bokov V A. Coexistence of magnetic and electric ordering in crystals. J Appl Phys, 1964, 35: 915—918
4 Qu W, Tan X, McCallum R W, et al. Room temperature magnetoelectric multiferroism through cation ordering in complex perovskite solid solutions. J Phys: Cond Matt, 2006, 18: 8935—8942
5 Bokov V A, Myl'nikova I E, Smolenskii G A. Ferroelectrics and antiferromagnetics. Zhurnal Eksperimental'noi i Teoreticheskoi Fiziki, 1962, 42: 643—646
6 Wongmaneerung R, Tan X, McCallum R W, et al. Cation, dipole, and spin order in $Pb(Fe_{2/3}W_{1/3})O_3$-based magnetoelectric multiferroic compounds. Appl Phys Lett, 2007, 90: 242905
7 Fiebig M. Revival of the magnetoelectric effect. J Phys D: Appl Phys, 2005, 38: R123—R152
8 Spaldin N A, Fiebig M. The renaissance of magnetoelectric multiferroics. Science, 2005, 309: 391—392
9 Eerenstein W, Mathur N D, Scott J F. Multiferroic and magnetoelectric materials, Nature, 2006, 442: 759—765
10 Tokura Y. Multiferroics—toward strong coupling between magnetization and polarization in a solid. J Magn Magn Mater, 2007, 310: 1145—1150
11 Ederer C, Spaldin N A. A new route to magnetic ferroelectrics. Nature Mater, 2004, 3: 849
12 Noda K, Nakamura S, Nagayama J, et al. Magnetic field and external-pressure effect on ferroelectricity in manganites: Comparison between $GdMnO_3$ and $TbMnO_3$. J Appl Phys, 2005, 97: 10C103
13 Kimura T, Ishihara S, Shintani H, et al. Distorted perovskite with e_g^1 configuration as a frustrated spin system. Phys Rev B, 2003, 68: 060403(R)
14 Goto T, Kimura T, Lawes G, et al. Ferroelectricity and giant magnetocapacitance in perovskite rare-earth manganites. Phys Rev Lett, 2004, 92: 257201
15 Lawes G, Harris A B, Kimura T, et al. Magnetically driven ferroelectric order in $Ni_3V_2O_8$. Phys Rev Lett, 2005, 95: 087205
16 Mostovoy M. Ferroelectricity in spiral magnets. Phys Rev Lett, 2006, 96: 067601
17 Kenzelmann M, Harris A B, Jonas S, et al. Magnetic inversion symmetry breaking and ferroelectricity in $TbMnO_3$. Phys Rev Lett, 2005, 95: 087206

18 Yamasaki Y, Sagayama H, Goto T, et al. Electric control of spin helicity in a magnetic ferroelectric. Phys Rev Lett, 2007, 98: 147204
19 Zhou J S, Goodenough J B. Unusual evolution of the magnetic interactions versus structural distortions in $RMnO_3$ perovskites. Phys Rev Lett, 2006, 96: 247202
20 Cohen R E, Krakauer H. Lattice dynamics and origin of ferroelectricity in $BaTiO_3$: Linearized-augmented-plane-wave total-energy calculations. Phys Rev B, 1990, 42: 6416—6423
21 Cohen R E. Origin of ferroelectricity in perovskite oxides. Nature, 1992, 358: 136—138
22 Kuroiwa Y, Aoyagi S, Sawada A, et al. Evidence for Pb-O covalency in tetragonal $PbTiO_3$. Phys Rev Lett, 2001, 87: 217601
23 Ravy S, Itie J P, Polian A, et al. High-pressure study of X-ray diffuse scattering in ferroelectric perovskites. Phys Rev Lett, 2007, 99: 117601
24 Hill N A. Why are there so few magnetic ferroelectrics? J Phys Chem B, 2000, 104: 6694—6709
25 Hill N A, Filippetti A. Why are there any magnetic ferroelectrics? J Magn Magn Mater, 2002, 242-245: 976—979
26 Baettig P, Ederer C, Spaldin N A. First principles study of the multiferroics $BiFeO_3$, Bi_2FeCrO_6, and $BiCrO_3$: Structure, polarization, and magnetic ordering temperature. Phys Rev B, 2005, 72: 214105
27 Tomashpol'skii Yu Y, Zubova E V, Burdina K P, et al. X-ray diffraction study of the ferromagnets bismuth-(III) manganese-(III) trioxide and bismuth-(III) bromium-(III) trioxide and their solid solutions prepared at high pressure. Izvestiya Akademii Nauk SSSR Neorganicheskie Materialy, 1967, 3(11): 2132—2134
28 Ishiwata S, Azuma M, Takano M, et al. High pressure synthesis, crystal structure and physical properties of a new Ni(II) perovskite $BiNiO_3$. J Mater Chem, 2002, 12: 3733—3737
29 Hill N A, Battig P, Daul C. First principles search for multiferroism in $BiCrO_3$. J Phys Chem B, 2002, 106: 3383—3388
30 Niitaka S, Azuma M, Takano M, et al. Crystal structure and dielectric and magnetic properties of $BiCrO_3$ as a ferroelectromagnet. Solid State Ionics, 2004, 172: 557—559
31 Moreau J M, Michel C, Gerson R, et al. Ferroelectric bismuth ferrite [$BiFeO_3$] X-ray and neutron diffraction study. J Phys Chem Solids, 1971, 32: 1315—1320
32 Michel C, Moreau J M, Achenbach G D, et al. The atomic structure of $BiFeO_3$. Solid State Comm, 1969, 7: 701—704
33 Kubel F, Schmid H. Structure of a ferroelectric and ferroelastic monodomain crystal of the perovskite $BiFeO_3$. Acta Crystallogr B, 1990, 46: 698—702
34 Maitre A, Francois M, Gachon J C. Experimental study of the Bi_2O_3-Fe_2O_3 pseudo-binary system. J Phase Equil Diff, 2004, 25: 59—67
35 Palai R, Katiyar R S, Schmid H, et al. β phase and β-γ metal-insulator transition in multiferroic $BiFeO_3$. Phys Rev B, 2008, 77: 014110
36 Fedulov S A, Venevtsev Yu, Zhdanov G S, et al. High temperature X-ray and thermographic studies of bismuth ferrite. Kristallografiya, 1961, 6: 795—796
37 Mukherjee J L, Wang F Y. Kinetics of solid-state reaction of Bi_2O_3 and Fe_2O_3. J Am Ceram Soc, 1971, 54: 31—34
38 Tabares-Munoz C, Rivera J P, Schmid H. Ferroelectric domains, birefringence and absorption of single crystals of $BiFeO_3$. Ferroelectrics, 1984, 55: 235—238
39 Achenbach G D, James W J, Gerson R. Preparation of single-phase polycrystalline $BiFeO_3$. J Am Ceram Soc, 1967, 50: 437
40 Lebeugle D, Colson D, Forget A, et al. Room-temperature coexistence of large electric polarization and magnetic order in $BiFeO_3$ single crystals. Phys Rev B, 2007, 76: 024116
41 Wang Y P, Zhou L, Zhang M F, et al. Room-temperature saturated ferroelectric polarization in $BiFeO_3$ ceramics synthesized by rapid liquid phase sintering. Appl Phys Lett, 2004, 84: 1731—1733
42 Lin Y H, Jiang Q H, Wang Y, et al. Enhancement of ferromagnetic properties in $BiFeO_3$ polycrystalline ceramic by La doping. Appl Phys Lett, 2007, 90: 172507
43 Roginskaya Y E, Venevtsev Y N, Fedulov S A, et al. X-ray investigations and study of magnetic and electrical properties of the system $BiFeO_3$-$LaFeO_3$. Kristallografiya, 1963, 8: 610—616
44 Das S R, Choudhary R N P, Bhattacharya P, et al. Structural and multiferroic properties of La-modified $BiFeO_3$ ceramics. J Appl Phys, 2007, 101: 034104
45 Yuan G L, Or S W. Enhanced piezoelectric and pyroelectric effects in single-phase multiferroic $Bi_{1-x}Nd_xFeO_3$ (x=0–0.15) ceramics. Appl Phys Lett, 2006, 88: 062905
46 Brinkman K, Iijima T, Takamura H. Acceptor doped $BiFeO_3$ ceramics: A new material for oxygen permeation membranes. Jpn J Appl Phys, 2007, 46: L93—L96
47 Shamir N, Gurewrrz E, Shaked H. The magnetic structure of $Bi_2Fe_4O_9$ — Analysis of neutron diffraction measurements. Acta Cryst A, 1978, 34: 662—666
48 Yuan G L, Or S W, Wang Y P, et al. Preparation and multi-properties of insulated single-phase $BiFeO_3$ ceramics. Solid State Comm, 2006, 138: 76—81
49 Pradhan A K, Zhang K, Hunter D, et al. Magnetic and electrical properties of single-phase multiferroic $BiFeO_3$. J Appl Phys, 2005, 97: 093903
50 Zhang S T, Lu M H, Wu D, et al. Larger polarization and weak ferromagnetism in quenched $BiFeO_3$ ceramics with a distorted rhombohedral crystal structure. Appl Phys Lett, 2005, 87: 262907
51 Su W N, Wang D H, Cao Q Q, et al. Large polarization and enhanced magnetic properties in $BiFeO_3$ ceramic prepared by high-pressure synthesis. Appl Phys Lett, 2007, 91: 092905
52 Rakov D N, Murashov V A, Bush A A, et al. Growth and pyroelectric properties of bismuth orthoferrite single crystals. Sov Phys Crystallogr, 1988, 33: 262
53 Yang H, Jain M, Suvorova N A, et al. Temperature-dependent leakage mechanisms of Pt/$BiFeO_3$/$SrRuO_3$ thin film capacitors. Appl Phys Lett, 2007, 91: 072911
54 Chen F, Zhang Q F, Li J H, et al. Sol-gel derived multiferroic $BiFeO_3$ ceramics with large polarization and weak ferromagnetism. Appl Phys Lett, 2006, 89: 092910
55 Yuan G L, Or S W, Chan H L W, et al. Reduced ferroelectric coercivity in multiferroic $Bi_{0.825}Nd_{0.175}FeO_3$ thin film. J Appl Phys, 2007, 101: 024106
56 Lee S U, Kim S S, Jo H K, et al. Electrical properties of Cr-doped $BiFeO_3$ thin films fabricated on the p-type Si (100) substrate by chemical solution deposition. J Appl Phys, 2007, 102: 044107
57 Pabst G W, Martin L W, Chu Y H, et al. Leakage mechanisms in $BiFeO_3$ thin films. Appl Phys Lett, 2007, 90: 072902
58 Sun J L, Li Y W, Li T X, et al. Electrical transport properties of

$BiFeO_3$ thin film. J Infrared Millim Waves, 2006, 25: 401—404
59 Naganuma H, Okamura S. Structural, magnetic, and ferroelectric properties of multiferroic $BiFeO_3$ film fabricated by chemical solution deposition. J Appl Phys, 2007, 101: 09M103
60 Clark S J, Robertson J. Band gap and Schottky barrier heights of multiferroic $BiFeO_3$. Appl Phys Lett, 2007, 90: 132903
61 Sun J L. Private Communication
62 Zhu J S, Lu X M, Jiang W, et al. Optical study on the size effects in $BaTiO_3$ thin films. J Appl Phys, 1997, 81: 1392—1395
63 Qi X, Dho J, Tomov R, et al. Greatly reduced leakage current and conduction mechanism in aliovalent-ion-doped $BiFeO_3$. Appl Phys Lett, 2005, 86: 062903
64 Chung C F, Lin J P, Wu J M. Influence of Mn and Nb dopants on electric properties of chemical-solution-deposited $BiFeO_3$ films. Appl Phys Lett, 2006, 88: 242909
65 Kumar M, Yadav K L. Study of room temperature magnetoelectric coupling in Ti substituted bismuth ferrite system. J Appl Phys, 2006, 100: 074111
66 Jun Y K, Moon W T, Chang C M, et al. Effects of Nb-doping on electric and magnetic properties in multiferroic $BiFeO_3$ ceramics. Solid State Comm, 2005, 135: 133—137
67 Singh S K, Maruyama K, Ishiwara H. Reduced leakage current in La and Ni codoped $BiFeO_3$ thin films. Appl Phys Lett, 2007, 91: 112913
68 Habouti S, Solterbeck C H, Es-Souni M. $LaMnO_3$ effects on the ferroelectric and magnetic properties of chemical solution deposited $BiFeO_3$ thin films. J Appl Phys, 2007, 102: 074107
69 Kim J K, Kim S S, Kim W J, et al. Substitution effects on the ferroelectric properties of $BiFeO_3$ thin films prepared by chemical solution deposition. J Appl Phys, 2007, 101: 014108
70 Tomashpol'skii Y Y, Skorikov V M, Venevtsev Y N, et al. Growth and some structure studies of single crystals of ferroelectric $BiFeO_3$. Izvestiya Akademii Nauk SSSR Neorganicheskie Materialy, 1966, 2(4): 707—711
71 Kubel F, Schmid H. Growth, twinning and etch figures of ferroelectric/ferroelastic dendritic bismuth iron oxide, $BiFeO_3$, single domain crystals. J Crystal Growth, 1993, 129: 515—524
72 Lebeugle D, Colson D, Forget A, et al. Very large spontaneous electric polarization in $BiFeO_3$ single crystals at room temperature and its evolution under cycling fields. Appl Phys Lett, 2007, 91: 022907
73 Neaton J B, Ederer C, Waghmare U V, et al. First-principles study of spontaneous polarization in multiferroic $BiFeO_3$. Phys Rev B, 2005, 71: 014113
74 Sosnowska I, Przenioslo R, Fischer P, et al. Investigation of crystal and magnetic structure of $BiFeO_3$ using neutron diffraction. Acta Phys Polonica A, 1994, 86: 629—632
75 Sosnowska I, Przenioslo R, Fischer P, et al. Neutron diffraction studies of the crystal and magnetic structures of $BiFeO_3$ and $Bi_{0.93}La_{0.07}FeO_3$. J Magn Magn Mater, 1996, 160: 384—385
76 Przenioslo R, Regulski M, Sosnowska I. Modulation in multiferroic $BiFeO_3$: Cycloidal, elliptical or SDW? Jpn J Phys Soc, 2006, 75(8): 084718
77 Katsura H, Nagaosa N, Balatsky A V. Spin current and magnetoelectric effect in noncollinear magnets. Phys Rev Lett, 2005, 95: 057205
78 Arkenbout A H, Palstra T T M, Siegrist T, et al. Ferroelectricity in the cycloidal spiral magnetic phase of $MnWO_4$. Phys Rev B, 2006, 74: 184431
79 Zalesskii A V, Frolov A A, Zvezdin A K, et al. Effect of spatial spin modulation on the relaxation and NMR frequencies of ^{57}Fe nuclei in a ferroelectric antiferromagnet $BiFeO_3$. J. Exp Theor Phys, 2002, 95: 101—105
80 Zalessky A V, Frolov A A, Khimich T A, et al. ^{57}Fe NMR study of spin-modulated magnetic structure in $BiFeO_3$. Europhys Lett, 2000, 50: 547—551
81 Sosnowska I, Zvezdin A K. Origin of the long period magnetic ordering in $BiFeO_3$. J Magn Magn Mater, 1995, 140: 167
82 Przenioslo R, Palewicz A, Regulski M, et al. Does the modulated magnetic structure of $BiFeO_3$ change at low temperatures? J Phys: Cond Matt, 2006, 18: 2069—2075
83 Bai F M, Wang J L, Wuttig M, et al. Destruction of spin cycloid in $(111)_c$-oriented $BiFeO_3$ thin films by epitiaxial constraint: Enhanced polarization and release of latent magnetization. Appl Phys Lett, 2005, 86: 032511
84 Wang J, Neaton J B, Zheng H, et al. Epitaxial $BiFeO_3$ multiferroic thin film heterostructures. Science, 2003, 299: 1719—1722
85 Li J B, Rao G H, Liang J K, et al. Magnetic properties of $Bi(Fe_{1-x}Cr_x)O_3$ synthesized by a combustion method. Appl Phys Lett, 2007, 90: 162513
86 Eerenstein W, Morrison F D, Dho J, et al. Comment on "Epitaxial $BiFeO_3$ multiferroic thin film heterostructures". Science, 2005, 307: 1203a
87 Béa H, Bibes M, Fusil S, et al. Investigation on the origin of the magnetic moment of $BiFeO_3$ thin films by advanced X-ray characterizations. Phys Rev B, 2006, 74: 020101
88 Siwach P K, Singh H K, Singh J, et al. Anomalous ferromagnetism in spray pyrolysis deposited multiferroic $BiFeO_3$ films. Appl Phys Lett, 2007, 91: 122503
89 Tabares-Munoz C, Rivera J P, Bezinges A, et al. Measurement of the quadratic magnetoelectric effect on single crystalline $BiFeO_3$. Jpn J Appl Phys, 1985, 24(Suppl. 24-2): 1051—1053
90 Popov Yu F, Kadomtseva A M, Vorobev G P, et al. Discovery of the linear magnetoelectric effect in magnetic ferroelectric $BiFeO_3$ in a strong magnetic field. Ferroelectrics, 1994, 162: 483—488
91 Popov Yu F, Kadomtseva A M, Krotov S S, et al. Features of the magnetoelectric properties of $BiFeO_3$ in high magnetic fields. Low Temp Phys, 2001, 27: 478—479
92 Kadomtseva A M, Popov Yu F, Pyatakov A P, et al. Phase transitions in multiferroic $BiFeO_3$ crystals, thin-layers, and ceramics: Enduring potential for a single phase, room-temperature magnetoelectric 'holy grail'. Phase Transitions, 2006, 79(12): 1019—1042
93 Ruette B, Zvyagin S, Pyatakov A P, et al. Magnetic-field-induced phase transition in $BiFeO_3$ observed by high-field electron spin resonance: Cycloidal to homogeneous spin order. Phys Rev B, 2004, 69: 064114
94 Kadomtseva A M, Popov Yu F, Vorob'ev G P, et al. Spin density wave and field induced phase transitions in magnetoelectric antiferromagnets. Physica B, 1995, 211: 327—330
95 Zhang S T, Pang L H, Zhang Y, et al. Preparation, structures, and multiferroic properties of single phase $Bi_{1-x}La_xFeO_3$ (x=0–0.40) ceramics. J Appl Phys, 2006, 100: 114108
96 Sosnowska I, Schfer W, Kockelmann W, et al. Crystal structure and

spiral magnetic ordering of $BiFeO_3$ doped with manganese. Appl Phys A, 2002, 74(Suppl): S1040—S1042
97 Kumar M M, Srinivas A, Kumar G S, et al. Investigation of the magnetoelectric effect in $BiFeO_3$-$BaTiO_3$ solid solutions. J Phys: Cond Matt, 1999, 11: 8131—8139
98 Kim J S, Cheon C I, Choi Y N, et al. Ferroelectric and ferromagnetic properties of $BiFeO_3$-$PrFeO_3$-$PbTiO_3$ solid solutions. J Appl Phys, 2003, 93: 9263—9270
99 Zalesskii A V, Frolov A A, Khimich T A, et al. Composition-induced transition of spin-modulated structure into a uniform antiferromagnetic state in a $Bi_{1-x}La_xFeO_3$ system studied using ^{57}Fe NMR. Phys Solid State, 2003, 45: 141—145
100 Murashov V A, Rakov D N, Ionov V M, et al. Magnetoelectric (Bi,Ln)FeO_3 compounds: crystal growth, structure, and properties. Ferroelectrics, 1994, 162: 359—369
101 Kaczmarek W, Polomska M, Pajak Z. Phase diagram of (bismuth lanthanum) ferrite ($(Bi_{1-x}La_x)FeO_3$) solid solution. Phys Lett A, 1974, 7: 227—228
102 Kamba S, Nuzhnyy D, Savinov M, et al. Infrared and terahertz studies of polar phonons and magnetodielectric effect in multiferroic $BiFeO_3$ ceramics. Phys Rev B, 2007, 75: 024403
103 Catalan G. Magnetocapacitance without magnetoelectric coupling. Appl Phys Lett, 2006, 88: 102902
104 Hill N A, Rabe K M. First-principles investigation of ferromagnetism and ferroelectricity in bismuth manganite. Phys Rev B, 1999, 59: 8759—8769
105 Sugawara F, Iida S, Shono Y, et al. New magnetic perovskites $BiMnO_3$ and $BiCrO_3$. Jpn J Phys Soc, 1965, 20: 1529
106 Sugawara F, Iida S, Shono Y, et al. Magnetic properties and crystal distortions of $BiMnO_3$ and $BiCrO_3$. Jpn J Phys Soc, 1968, 25: 1553—1558
107 Kimura T, Kawamoto S, Yamada I, et al. Magnetocapacitance effect in multiferroic $BiMnO_3$. Phys Rev B, 2003, 67: 180401
108 Sharan A, Lettieri J, Jia Y, et al. Bismuth manganite: A multiferroic with a large nonlinear optical response. Phys Rev B, 2004, 69: 214109
109 Belik A A, Iikubo S, Yokosawa T, et al. Origin of the monoclinic-to-monoclinic phase transition and evidence for the centrosymmetric crystal structure of $BiMnO_3$. J Am Chem Soc, 2007, 129: 971—977
110 Montanari E, Calestani G, Righi L, et al. Structural anomalies at the magnetic transition in centrosymmetric $BiMnO_3$. Phys Rev B, 2007, 75: 220101
111 Baettig P, Seshadri R, Spaldin N A. Anti-polarity in ideal $BiMnO_3$. J Am Chem Soc, 2007, 129: 9854—9855
112 Atou T, Chiba H, Ohoyama K, et al. Structure determination of ferromagnetic perovskite $BiMnO_3$. J Solid State Chem, 1999, 145: 639—642
113 Santos A M, Cheetham A K, Atou T, et al. Orbital ordering as the determinant for ferromagnetism in biferroic $BiMnO_3$. Phys Rev B, 2002, 66: 064425
114 Baettig P, Spaldin N A. *ab initio* prediction of a multiferroic with large polarization and magnetization. Appl Phys Lett, 2005, 86: 012505
115 Suchomel M R, Thomas C I, Allix M, et al. High pressure bulk synthesis and characterization of the predicted multiferroic $Bi(Fe_{1/2}Cr_{1/2})O_3$. Appl Phys Lett, 2007, 90: 112909
116 Nechache R, Harnagea C, Pignolet A, et al. Growth, structure, and properties of epitaxial thin films of first-principles predicted multiferroic Bi_2FeCrO_6. Appl Phys Lett, 2006, 89: 102902
117 Kim D H, Lee H N, Biegalski M D, et al. Large ferroelectric polarization in antiferromagnetic $BiFe_{0.5}Cr_{0.5}O_3$ epitaxial films. Appl Phys Lett, 2007, 91: 042906
118 Nechache R, Harnagea C, Gunawan L, et al. Growth, structure, and properties of $BiFeO_3$-$BiCrO_3$ films obtained by dual cross beam PLD. IEEE Trans Ultras Ferroelect Freq Contr, 2007, 54: 2645—2652
119 Yu J, Itoh M. Searching for novel single phase magnetoelectric materials: their magnetic properties. In: The MRS Fall Meeting, 2005, abstract No. U6.6
120 Yu J. Designing novel high temperature single-phase magnetoelectric materials. In: Fall Meeting of Chinese Physical Society, Nanjing University, 2007
121 Anderson P W. Antiferromagnetism. Theory of superexchange interaction. Phys Rev, 1950, 79: 350—356
122 Goodenough J B. Magnetism and the Chemical Bond. New York: Interscience, 1963
123 Kanamori J. Superexchange interaction and symmetry properties of electron orbitals. J Phys Chem Solids, 1959, 10: 87—98
124 Goodenough J B, Wold A, Arnott R J, et al. Relationship between crystal symmetry and magnetic properties of ionic compounds containing Mn^{3+}. Phys Rev, 1961, 124: 373—384
125 Imada M, Fujimori A, Tokura Y. Metal-insulator transitions. Rev Mod Phys, 1998, 70: 1039—1263
126 Goodenough J B. Theory of the role of covalence in the perovskite-type manganites [La,M(II)]MnO_3. Phys Rev, 1955, 100: 564—573
127 Bokov V A, Grigoryan N A, Bryzhina M F, et al. Effect of lattice distortions on the magnetic behavior of perovskite-type manganites. Phys Stat Sol, 1968, 28: 835—847
128 Troyanchuk I O, Samsonenko N V, Shapovalova E F, et al. Magnetic phase transitions in the bismuth-containing manganates with perovskite structure. J Phys: Cond Matt, 1996, 8: 11205—11212
129 Goodenough J B. Localized versus collective *d* electrons and Néel temperatures in perovskite and perovskite-related structures. Phys Rev, 1967, 164: 785—789
130 Kimura T, Lawes G, Goto T, et al. Magnetoelectric phase diagrams of orthorhombic $RMnO_3$ (R=Gd, Tb, and Dy). Phys Rev B, 2005, 71: 224425
131 Terakura K. Magnetism, orbital ordering and lattice distortion in perovskite transition-metal oxides. Prog Mater Sci, 2007, 52: 388—400
132 Heikes R R. Relation of magnetic structure to electrical conductivity in NiO and related compounds. Phys Rev, 1955, 99: 1232—1234
133 Urushibara A, Moritomo Y, Arima T, et al. Insulator-metal transition and giant magnetoresistance in $La_{1-x}Sr_xMnO_3$. Phys Rev B, 1995, 51: 14103—14109